

Development and Validation of EBRDYN code by Benchmark Analysis of EBR-II SHRT-17 Test

Partha Sarathy U.¹, Velusamy K.¹ and Puthiyavinayagam P.¹

¹Indira Gandhi Centre for Atomic Research, Kalpakkam, India

E-mail contact of main author: ups@igcar.gov.in

Abstract. Experimental Breeder Reactor (EBR-II) was a U-Pu-Zr metal-alloy fueled liquid-metal-cooled fast reactor, extensively used for conducting safety experiments. Out of several tests conducted, the SHRT-17 loss of flow test conducted in 1984 demonstrated the decay heat removal capability by natural circulation in sodium cooled fast reactor with no core damage. In order to utilize the data recorded during these tests for improving the computer codes by extensive code validation, IAEA has initiated a coordinated Research Project (CRP) in which IGCAR, INDIA is one of the participants. IGCAR has developed a plant dynamics code EBRDYN, on the same principles as Indian safety codes FBRDYN, DYANA-P and DHDYN used for the safety analysis of Indian Fast Reactors FBTR and PFBR. The EBRDYN consists of thermal hydraulic models of various components of EBR-II primary heat transport system viz., core, hot upper plenum, Z-pipe, intermediate heat exchanger (IHX), cold pool, primary sodium pumps and associated piping. All the subassemblies (SA) of the core are grouped into a convenient number of radial zones receiving sodium from bottom plenum and discharging into the top hot plenum. The mixing of sodium in the upper plenum, dynamics of Z-pipe, heat transfer in IHX from primary to the intermediate sodium etc., have been modeled. The primary sodium pumps have been modeled using homologous characteristics and with previous EBR-II experience. The pump models are capable of handling negative flows. The primary sodium circuit has been modeled with the capability to handle two primary pumps operating in parallel. The initial conditions of the reactor and transient boundary conditions viz., core decay power, primary pumps speed, IHX secondary sodium flow rate and inlet temperature as provided by Argonne National Laboratory (ANL) have been used. The steady state and transient results are compared against measured data. The paper gives details of thermal hydraulic modeling of the primary heat transport system, the transient results and their comparison with the measured data.

Key Words: EBR-II, SHRT-17, Natural Convection, EBRDYN.

1. Introduction

EBR-II was 62.5 MWth, 20 MWe, Uranium-Plutonium metal-fuelled experimental fast breeder reactor operated from 1964 to 1994 at Idaho national Laboratory, USA [1]. This was a heavily instrumented reactor in which several safety related Shutdown Heat Removal Tests (SHRT) were carried out during its last 15 years of life time. In order to bring the benefit of these tests to international fast reactor community to validate simulation tools and models for safety analysis of sodium cooled fast reactors, IAEA in collaboration with ANL, USA had initiated a Coordinated Research Project (CRP), 'Benchmark Analyses of an EBR-II Shutdown Heat Removal Test' for benchmarking the SHRT-17 and SHRT-45R tests. The important input data for developing the code viz., reactor geometry, steady state plant parameters, transient decay heat generation data, IHX intermediate inlet temperature and flow rate are supplied by ANL. The data to be generated by the code are the peak in-core coolant temperature, peak clad temperature, peak fuel temperature, high pressure plenum temperature, low pressure plenum temperature, Z-pipe inlet temperature, IHX inlet and outlet temperatures and sodium flow rates. Towards this goal, a 1-D plant dynamics code EBRDYN has been developed and the SHRT-17 test has been simulated. The paper discusses the details of mathematical models, computational schemes used, results obtained from the simulation.

2. System Description

The EBR-II was a sodium-cooled, single-pool-type fast reactor, with three coupled heat transport circuits viz., primary sodium circuit, secondary sodium circuit and steam-water system with rated flow rates of 485 kg/s, 315 kg/s and 32 kg/s respectively. A schematic of the EBR-II plant is shown in Fig. 1. All major primary system components were submerged in the primary tank, which contained $\sim 340 \text{ m}^3$ of liquid sodium at 371°C [2]. Two primary pumps drew sodium from this pool and provided sodium to the two inlet plena for the core. Subassemblies in the inner core and extended core regions received sodium from the high-pressure inlet plenum, accounting for approximately 85% of the total primary flow. The blanket and reflector subassemblies in the outer blanket region received sodium from the low-pressure inlet plenum. Hot sodium exited the subassemblies into a common upper plenum where it mixed before passing through the outlet pipe into the intermediate heat exchanger (IHX). The outlet pipe feeding sodium to the IHX is referred to as the 'Z-pipe'. Sodium then exited the IHX back into the primary tank before entering the primary sodium pumps again. The hot sodium while passing through the IHX transferred heat to the cold intermediate sodium. The IHX was a shell and tube type heat exchanger with primary sodium flowing on shell side and intermediate sodium flowing on tube side. Each primary pump is powered by a variable speed motor-generator in which the pump speed is controlled by varying the current [3]. The intermediate sodium transferred heat to the balance-of-plant while flowing through the steam generator. EBR-II was heavily instrumented to measure mass flow rates, temperatures and pressures throughout the system.

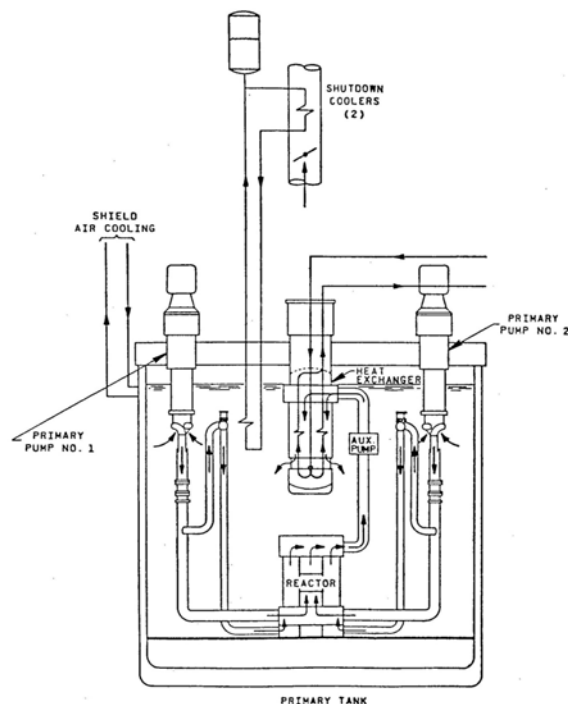


FIG. 1. EBR-II Primary tank sodium flow paths

3. Description of the Test

EBR-II started power operation in 1964 and the reactor was shut-down in 1994. A series of experiments involved in reactor shutdown tests, known as SHRTs, demonstrated the passive decay heat removal by natural circulation of primary sodium coolant. SHRT-17 was a full power loss-of-flow test conducted on June 20, 1984. Prior to the start of the test, EBR-II was operated at full power (57.3 MWt) and full flow 456 kg/s to bring the system to an equilibrium state. The core inlet temperature was 351.5°C . The IHX secondary sodium inlet temperature was 301.12°C and the flow rate was 311.7 kg/s. The SHRT-17 transient was initiated by a trip of the primary and intermediate pumps. The reactor was also instantaneously scrammed. Each primary pump had its own controller and motor-generator (M-G set). The flow coastdown was governed by the kinetic energy stored in the inertia of the M-G set. The two pump drive units had intrinsic differences which caused a difference in stop times. As the SHRT-17 test continued, the reactor decay power decreased due to fission product decay. After the start of the test, no automatic or operator action took place until the

test had concluded. During the test, reactor inlet, reactor outlet, IHX primary inlet, IHX intermediate outlet temperatures and the pressures at the pump outlet and upper plenum were measured.

4. Modeling Details

4.1 Geometry/discretization

The nodalization of EBR-II primary heat transport system in EBRDYN is shown in Fig. 1. The core subassemblies receiving sodium from bottom high pressure plenum have been grouped into 9 radial zones. The first two zones represent fuel SA, the third zone represents inner blanket SA. The fourth and fifth zones represent the control rods and safety rods respectively. The sixth and seventh zones represent special instrumented SA XX09 and XX10 respectively. The eighth and ninth zones represent rest of the SA receiving sodium from the high pressure plenum. The tenth zone represents outer blanket /reflector subassemblies which receive sodium from low pressure inlet plenum. One representative SA from each zone has been modeled with 20 axial nodes and 4 radial nodes. The upper plenum, high pressure and low pressure inlet plenums and primary tank are modeled as perfect mixing volumes. The IHX is modeled as shell and tube heat exchanger and the details are given in section 4.5. The leakage flows from high pressure plenum and upper plenum to primary tank are also modeled.

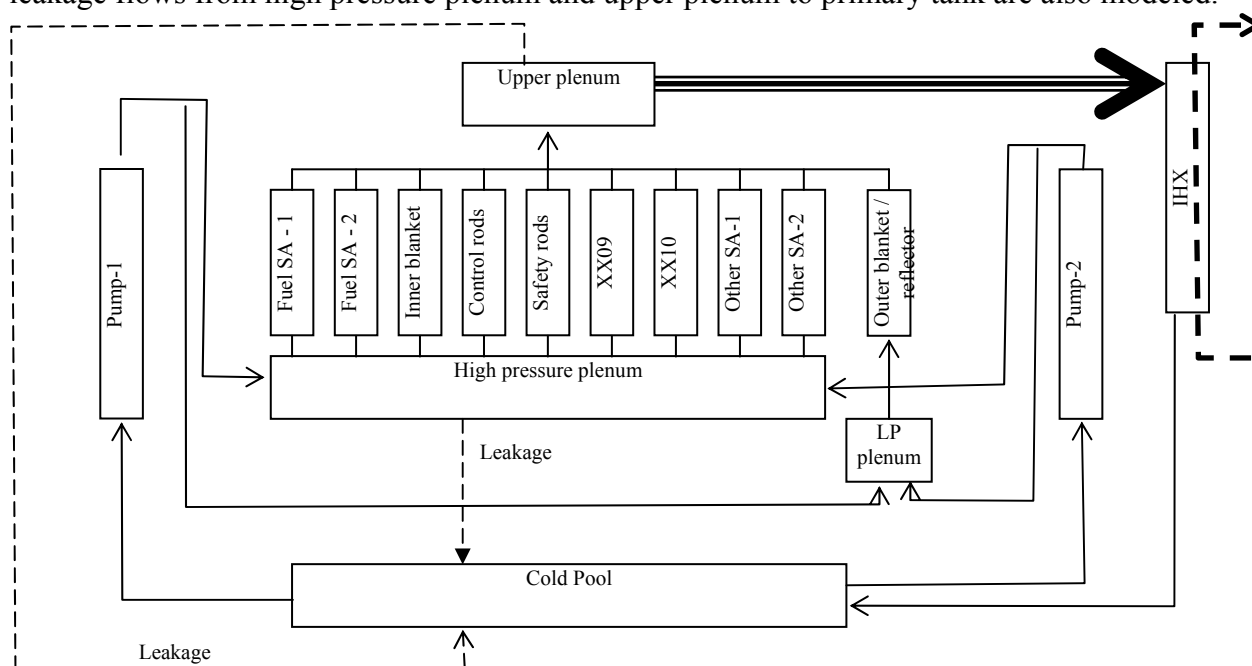


FIG. 2. EBRDYN modeling for the EBR-II

4.2 Basic Method

The important assumptions made are (i) Liquid sodium is assumed to be incompressible, (ii) Flow of sodium is treated as one dimensional through the pipelines, subassemblies, heat exchanger tubes etc., (iii) Axial conduction heat transfer in coolant pipe material, heat exchanger tubes and fuel pin, clad walls are neglected in comparison to the radial conduction. In addition to these, there are several specific assumptions made in deriving the individual component model and numerical schemes to solve them. The following sections present the description of individual models and specific assumptions made.

4.3 Fuel Subassembly

For the purpose of thermal and hydraulic analysis, one representative SA from each zone is modeled. The subassembly is divided into 20 axial zones – 1 zone for the lower shield part, 2 zones for bottom part of the pin, 10 zones for the active fuel length, 2 zones for top part of the pin and 5 zones for upper shield portion. In each axial zone, the thermal capacities of all the fuel, steel and sodium are separately lumped together and four heat exchanging nodes are formed, each described by a mean temperature. Two nodes are allotted for fuel pellets and one each for steel and sodium (Fig. 3). Then through the application of energy balance for each of the axial zones, four coupled ordinary differential equations in time are obtained. Solving them simultaneously in a sequential manner from the bottom to top of the subassembly gives the axial distribution of the sodium, clad and fuel temperatures in steady state and transient conditions. The decay power generated in the core is distributed amongst the subassemblies based on the steady state power distribution.

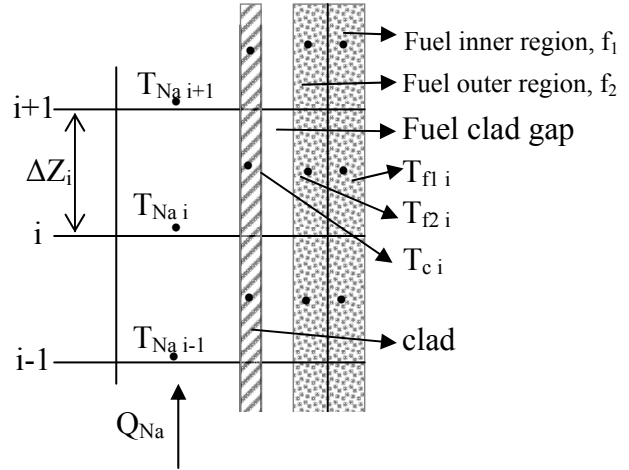


FIG. 3. Fuel pin model

The other important features of the model are:

- The thermal capacity of subassembly sheath steel is clubbed with clad steel.
- Inter subassembly heat transfer is not considered.
- Radial heat transfer phenomenon in the shielding and control rod subassemblies is not considered.

The working equations are as given below:

$$C_{f1i} \frac{dT_{f1i}}{dt} = 0.5P_i + h'_{f1f2} \cdot \delta Z_i (T_{f2i} - T_{f1i}) \quad (1)$$

$$C_{f2i} \frac{dT_{f2i}}{dt} = 0.5P_i + h'_{f1f2} \cdot \delta Z_i (T_{f1i} - T_{f2i}) + h'_{fc} \cdot \delta Z_i (T_{ci} - T_{f2i}) \quad (2)$$

$$C_{ci} \frac{dT_{ci}}{dt} = h'_{fc} \cdot \delta Z_i (T_{f2i} - T_{ci}) - h'_{cNa} \cdot \delta Z_i (T_{ci} - \bar{T}_i) \quad (3)$$

$$C_{Nai} \frac{dT_{Nai+1}}{dt} = (Qc_p)_{Na} (T_{Nai} - T_{Nai+1}) + h'_{cNa} \cdot \delta Z_i (T_{ci} - \bar{T}_i) \quad (4)$$

$$\text{with } \bar{T}_i = 0.5(T_{Nai} + T_{Nai+1}) \text{ and } \delta Z_i = Z_{i+1} - Z_i \quad (5)$$

$$C_{f1i} = C_{f2i} = 0.5 N_p \left(\frac{\pi}{4} d_p^2 \cdot \delta Z_i \cdot \rho_{fu} \cdot c_{p fu} \right) \quad (5)$$

$$C_{Nai} = S_{Nai} \cdot \delta Z_i \cdot \rho_{Na} \cdot c_{p Na} \quad (6)$$

$$C_{ci} = S_{sti} \cdot \delta Z_i \cdot \rho_{st} \cdot c_{p st} \quad (7)$$

$$h'_{f1f2} = 4 \cdot \pi \cdot k_{fu} \cdot N_p \quad (8)$$

$$h'_{fc} = U_{fc} \cdot \pi \cdot d_o \cdot N_p \quad (9)$$

$$\text{with } U_{fc} = \left[\frac{d_o}{8k_{fu}} + \frac{1}{h_g} \frac{d_o}{d_g} + \frac{d_o \ln\left(\frac{d_m}{d_i}\right)}{2k_{st}} \right]^{-1} \quad (10)$$

$$\text{and } h'_{cNa} = U_{cNa} \pi d_o N_p \quad (11)$$

$$\text{with } U_{cNa} = \left[\frac{d_o \ln\left(\frac{d_o}{d_m}\right)}{2k_{st}} + \frac{1}{h_{Na}} \right]^{-1}$$

For steady state solution, the time derivatives are equated to zero and the resulting equations are solved simultaneously. The transient solution of the above system of equations is obtained by a semi-implicit finite difference formulation as follows and solving them simultaneously:

$$\frac{dT_i}{dt} = \frac{T_i^j - T_i^{j-1}}{\Delta t} \quad \text{in the LHS and} \quad (12)$$

$$T_i = 0.5(T_i^j + T_i^{j-1}) \quad \text{in the RHS where } j \text{ is the index for time} \quad (13)$$

4.4 Sodium Plenums

The upper plenum, lower plenum and cold pool are modeled as perfect mixing volumes. For the upper plenum, the 10 zones flows and sodium outlet temperatures are the inputs and the mixed mean temperature is the output which is the inlet temperature for Z pipe. The leakage flow from upper plenum to the primary tank and reverse flows in SA also form outlets for the upper plenum. Similar approach is followed for lower plenum and primary tank. The working equations are given in

$$C_{up} \frac{dT_{up}}{dt} = \sum_{i=1}^n n_i Q_i c_p T_{SAO} - \sum_{i=1}^n n_i Q_{ir} c_p T_{up} - Q_l c_p T_{up} - Q_{lk1} c_p T_{up} \quad (14)$$

$$C_{PT} \frac{dT_{PT}}{dt} = Q_l c_p (T_{IO} - T_{PT}) + Q_{lk1} c_p T_{up} + Q_{lk2} c_p T_{lp} \quad (15)$$

where $Q_i = 0$ if the SA flow is positive and $Q_{ir} = 0$ if the SA flow is negative

Q_l is the IHX flow, Q_{lk1} and Q_{lk2} are the leakage flows from upper and lower plenums

4.5 IHX Thermal Model

This model evaluates the steady state and transient temperature profiles of the IHX primary and secondary sodium sides with respective flows and inlet temperatures as input. A two zone radial lumped one dimensional model with a single temperature for the primary sodium and intermediate sodium is used (Fig. 5). The shell is assumed to be at primary sodium temperature. The thermal capacity of the shell material is clubbed with that of the primary sodium. The thermal capacity of the tube material is clubbed with the primary sodium and secondary sodium equally. These assumptions lead to a set of two coupled hyperbolic partial differential equations. For the numerical solution of these basic

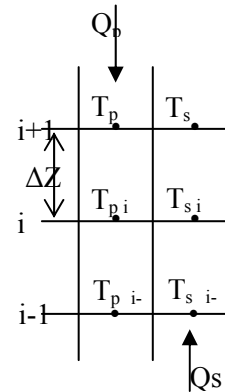


FIG. 5. IHX model

equations, the active length of the heat transfer region is divided into 40 regions. Then the equations are integrated with respect to length over these regions and a set of ordinary differential equations in time are obtained. These equations are discretized using nodal heat balance scheme incorporating the weighted mean temperature in the heat transfer term. The IHX primary outlet temperature and flow are the inputs for the cold pool calculations. The working equations are given below:

$$C_{pi} \frac{dT_{pi}}{dt} = Q_p c_p (T_{pi+1} - T_{pi}) + (UA_o)_i (\bar{T}_{si} - \bar{T}_{pi}) \quad (16)$$

$$C_{si} \frac{dT_{si+1}}{dt} = Q_s c_p (T_{si} - T_{si+1}) + (UA_o)_i (\bar{T}_{pi} - \bar{T}_{si}) \quad (17)$$

$$\text{where } \bar{T}_{pi} = fT_{pi+1} + (1-f)T_{pi} \quad (18)$$

$$\bar{T}_{si} = fT_{si+1} + (1-f)T_{si} \quad (19)$$

f is the weight factor given based on the thermal capacity of primary and secondary flows

$$(UA_o)_i = (A_o)_i \left[\frac{1}{h_p} + \frac{d_{To} \ln\left(\frac{d_{To}}{d_{Ti}}\right)}{2k_T} + \frac{d_{To}}{d_{Ti} h_s} \right]^{-1} \quad (20)$$

$$\text{with } (A_o)_i = N_T \pi d_{To} \delta Z_i \quad (21)$$

The steady state solution is obtained through solving the set of two simultaneous equations resulting from setting the time derivatives in the equations above to zero, in sequence from the bottom of the heat exchanger. If the heat exchanger is in counter-current mode, an iterative procedure is must. If the heat exchanger is in co-current mode, the outlet temperatures of each pair of volumes can be obtained by carrying out the calculations from the end in which both flows are entering without any iterations. The transient solution of the above system of equations is obtained by a semi-implicit finite difference formulation as given in Eqns.(12&13). By this procedure the ODE are reduced to a set of twin simultaneous equations for each pair of volume.

4.6 Z Pipe Thermal Model

The temperature changes that occur in the outlet of upper plenum are carried to the IHX inlet by the primary sodium flow through 'Z' pipe. This pipe line due to its considerable length, delay the transportation of the temperature changes to the other end. This delay is directly proportional to the mass velocities and thus they are capable of wide variation in a flow transient. To model these features it was found that a nodal heat balance type of approach is most convenient and computationally fast. The Z pipe is modelled as a double walled sodium carrying pipe dipped in primary tank with stagnant sodium in the annular gap. The total length of pipe line is divided into a finite number of regions with equal length. In each part, the primary sodium, inner pipe, stagnant sodium and outer pipe are represented by four nodes respectively (Fig. 4). The heat transfer from outer surface has been accounted. The governing equations are written by energy balance. Then this set of equations permit a sequential solution of the mesh temperatures from the knowledge of the inlet

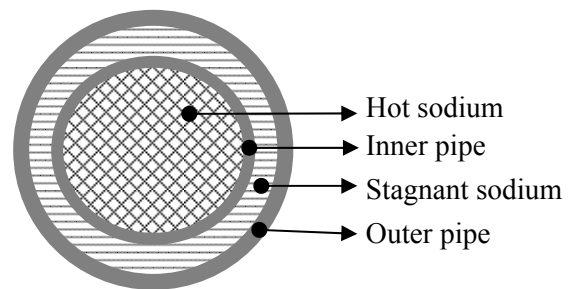


FIG. 4. Z Pipe model

temperatures. The heat transfer coefficient on the inside walls is calculated using forced convection correlations based on whether the flow is in laminar or turbulent regime. The Z pipe sodium outlet temperature and flow rate form the inputs for the IHX calculations.

4.7 Hydraulics

This part computes the steady state and transient hydraulics in the primary sodium system. The solution of this is decoupled from the thermal calculations on the assumption that the hydraulics is not a strong function of the temperature distribution. Nevertheless to make a good estimation of the natural convection effects, the buoyancy head terms in the model equations are estimated from the most recently updated temperature distributions. The effect of radial pressure distribution in the inlet plenum is neglected.

4.8 Core Hydraulics Model

All the SA zones are treated as parallel channels. The pressure drop coefficient for each SA is calculated based on the pressure drop across the core and the flow through the SA. The modeling has been carried out taking care of any possible reverse flows in some of the SA. To make a good estimation of the natural convection effects, the buoyancy head terms in the model equations are estimated from the most recently updated temperature distributions.

4.9 Pump Model

Pump speed as a function of time is taken from the input data and head is calculated using the equation:

$$\bar{H} = b_1 \bar{s}^{-2} + b_2 \bar{s} \bar{Q} + b_3 \frac{\bar{Q}}{|\bar{Q}|} |\bar{Q}|^{b_4} \quad (22)$$

$$\text{where} \quad \bar{H} = \frac{H}{H_r} \quad \bar{s} = \frac{s}{s_r} \quad \bar{Q} = \frac{Q}{Q_r} \quad (23)$$

H = pump head, s = pump speed and Q = coolant flow rate. The r subscript refers to the rated value. The coefficients $b_1 = 1.1740$ and $b_2 = 0.0818$ and b_3 and b_4 values depend on the speed and flow rate, plus several empirical constants [2].

5. Boundary Conditions

For steady state calculations, the primary pump flow, pump speed, primary flow through various SA, reactor inlet, normalized power distribution in the SA, intermediate sodium flow of IHX and its inlet temperature are inputs. For transient calculations the core decay power, primary pump speed, IHX intermediate sodium flow and its inlet temperature are the boundary conditions. Data is provided for each of the boundary conditions for the 15-minute duration of the test. Figure 5&6 show the pump speeds and core power as function of time. Figures 7 and 8 show the IHX intermediate inlet temperature and flow rate as function of time

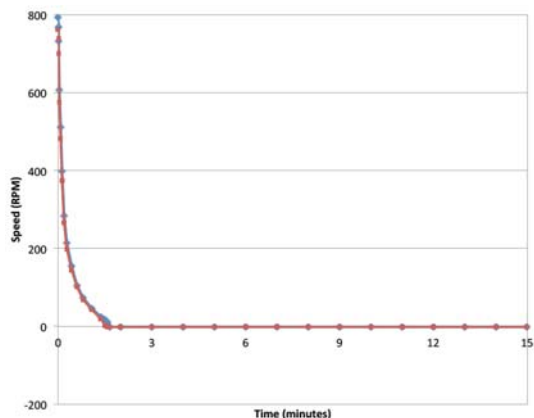


FIG. 5. Pumps speed during test

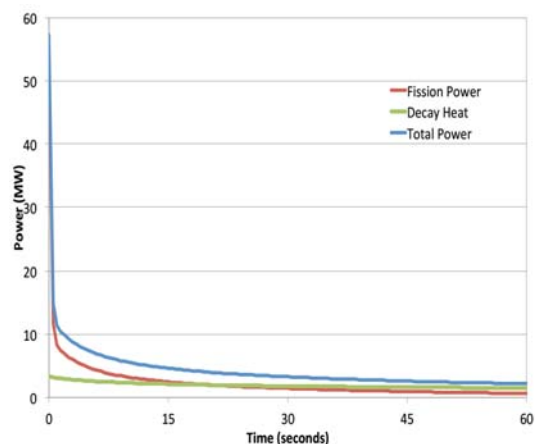


FIG. 6. Total, fission and decay heat during test

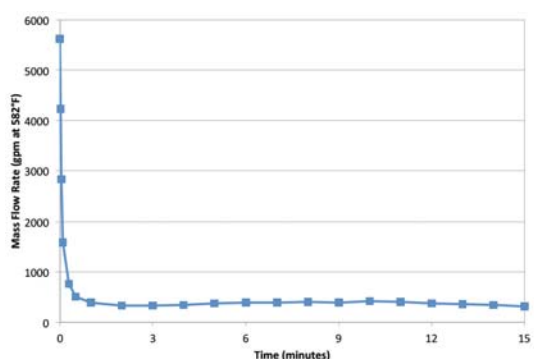


FIG. 7. IHX intermediate flow rate

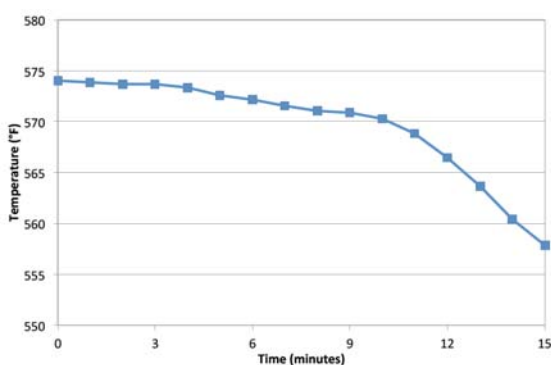


FIG. 8. IHX intermediate inlet temperature

6. Results and Discussion

6.1 Steady State Results

The reactor power is taken as 57.3 MW (including initial decay heat power of 3.36 MW). The core power is distributed amongst all the SA according to the normalized benchmark data. The speeds of pumps 1 & 2 are taken as 799 rpm and 765 rpm respectively. The intermediate sodium loop mass flow rate is taken as 312 kg/s with IHX intermediate inlet temperature as 574 K (301 °C). The pump flows are obtained as 255 kg/s and 215 kg/s respectively. The core inlet and outlet temperatures are obtained as 624.8 K (351.8 °C) and 735.7 K (462.7 °C) respectively. The IHX primary inlet and outlet temperatures are obtained as 721.7 K (448.7 °C) and 624.3 K (351.3 °C) respectively. The IHX secondary sodium outlet temperature is obtained as 713.4 K (440.4 °C).

6.2 Transient Results

Figure 9 shows the evolution of pump #1 and pump #2 flows. It can be seen that the pump #1 flow reverses for a short duration around 40 s. Figure 10 shows the evolution of core inlet temperature. It can be seen that the core inlet temperature initially remains constant at 624.8 K and reduces gradually to 623.3 K in 900 s. Figure 11 shows that the peak fuel and clad temperatures go to a maximum of 904 K at 65 s. The peak coolant temperature goes to a maximum of 888 K at 60 s. Figures 12-14 show the evolution of Z pipe inlet, IHX primary inlet and IHX secondary outlet temperatures respectively. It can be seen that the Z pipe inlet temperature goes to a minimum of 668 K at 20 s, goes to a maximum of 753 K (106 s) and comes down to 678 K in 900 s. The IHX primary inlet temperature closely follows the core

outlet temperature. The IHX secondary outlet temperature goes to a maximum of 728 K in 120 s and cools down to 662 K in 900 s. It can be seen that all the temperatures are predicted reasonably well except the IHX primary inlet temperature. The reason for this is not understood. Also the measured IHX secondary outlet temperature remained constant during the initial 100 s whereas the predicted temperature decreases to about 674 K and comes back to 728 K within 90 s. This deviation from prediction also could not be explained.

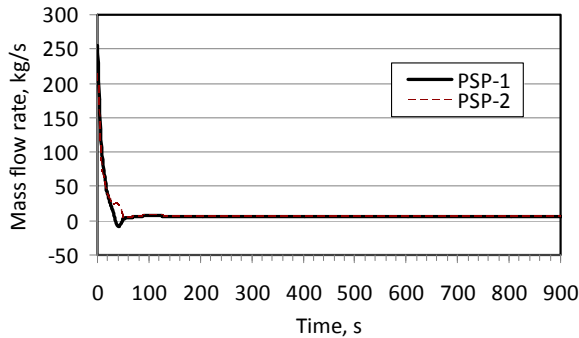


FIG. 9. Primary sodium pump flow

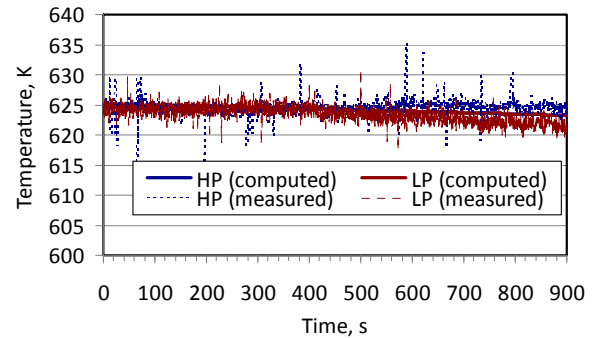


FIG. 10. Core inlet temperatures (High pressure & Low pressure)

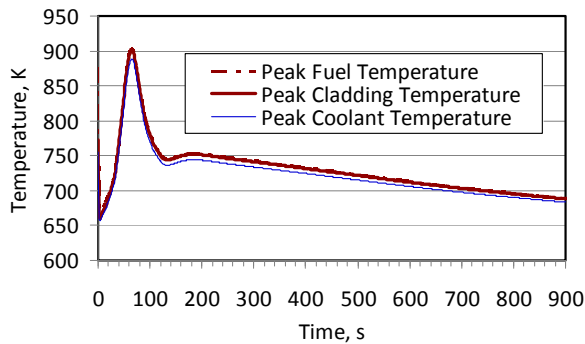


FIG. 11. Peak in-core temperatures

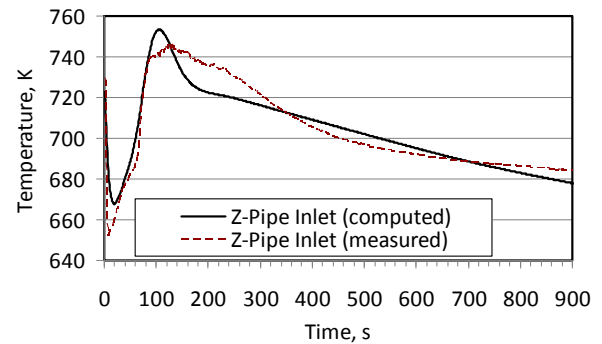


FIG. 12. Z pipe inlet temperature

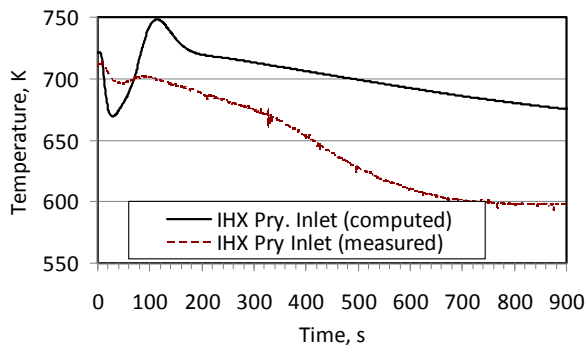


FIG. 13. IHX primary inlet temperature

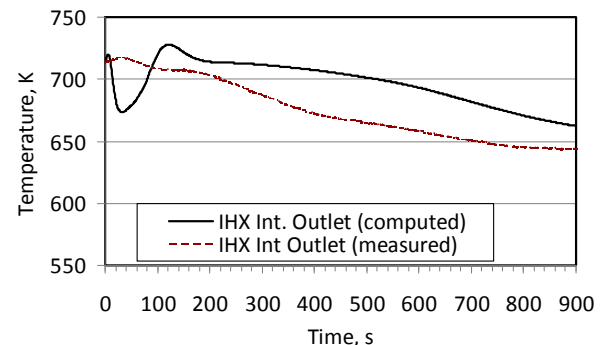


FIG. 14. IHX intermediate outlet temperature

7. Conclusion

The EBR-II primary heat transport system has been modeled using EBRDYN an in-house developed 1-D plant dynamics code. The code has been developed on the same principles as Indian fast reactor safety codes. The code predicted the steady state temperatures, flow rates very close to the measured values. The transient pump flow rates, reactor inlet and outlet temperatures are predicted very close to the measured values. This validates the EBRDYN code for simulating natural circulation decay heat removal conditions.

8. Nomenclature

A	Surface area, m ²	k	Thermal conductivity, Wm ⁻¹ K ⁻¹
c _p	Specific heat, Jkg ⁻¹ K ⁻¹	N	Number of pins/tubes
C	Thermal capacity of the volume under consideration, JK ⁻¹	P	Power, W
C'	Thermal capacity per unit length, JK ⁻¹ m ⁻¹	Q	Mass flow rate kg/s ⁻¹
d _p	Fuel pellet diameter, m	s	Pump speed, rpm
d _o	Fuel pin clad outer dia, m	S	Area of crosssection
d _i	Fuel pin clad inner diameter, m	T	Temperature, K
d _m	Fuel pin mean clad diameter, m	U	Overall heat transfer coefficient, W/(m ² K)
h'	Heat transmittance rate per unit length, Wm ⁻¹ K ⁻¹	δZ	Mesh length, m
H	Pump head, Pa		

Subscripts

c	clad	lk	leak
f1	Fuel pin central region	m	mean
f2	Fuel pin second region	Na	sodium
f1f2	Fuel central to second region	o	Outer or outlet
fc	Fuel to clad	p	pins
fu	fuel	PT	Primary tank
g	Argon gap	r	Reverse or reverse
i	Index for node or zone	st	steel
I	IHX	T	tube
j	Index for time	up	Upper plenum

9. References

- [1] Lehto, W.K., Dean, E.M., Fryer, R.M., "Reactor safety implications of pump runup tests in EBR-II", Nuclear Engineering and Design, Volume 110 (1), pp. 47-53, (1988).
- [2] Sumner, T., Wei, T.Y.C., "Benchmark Specifications and Data Requirements for EBR II Shutdown Heat Removal Tests SHRT 17 and SHRT 45R", Nuclear Engineering Division Argonne National Laboratory. ANL-ARC-226-(Rev 1), (2012).
- [3] Lehto, W.K., Fryer, R.M., Dean, E.M., Koenig, J.F., Chang, L.K., Mohr, D., Feldman, E.E., "Safety analysis for the loss-of-flow and loss-of-heat sink without scram tests in EBR-II" Nuclear Engineering and Design, Volume 101 (1), pp. 35-44(1987).